

# An Experimental Study of the Carbon-Fiber-Reinforced Plastics (CRFP) in Turning

Chung-Shin Chang

Professor, Department of Mechanical and Mechatronic Engineering, National Ilan University, Taiwan, R.O.C. 26041

## Abstract

In this paper, the machinability of high-strength CFRP materials in turning with chamfered main cutting edge of P and K type carbide tools has been investigated experimentally. The cutting forces, chip formation mechanism and the tool wear have been observed with respect to tip's geometries. Special tool holders were designed and manufactured at first, and then these holders with the mounting tip's were grinded to various tool geometries, including varying the width of chamfered main cutting edge, the side cutting edge angle, first and second side rake angle and back rake angle, etc. In this study, the smallest cutting force was achieved by using chamfered main cutting edge tool with  $C_s = 20^\circ$ ,  $\alpha_{s1}(\alpha_{s2}) = -10^\circ(10^\circ)$  and  $R = 0.1mm$ . K type is better than P type of chamfered main cutting edge tools.

**Keywords:** Turning, carbon fiber reinforced plastics (CFRP), and chamfered main cutting edge

# 碳纖維複合材料之車削加工研究

張充鑫

國立宜蘭大學機械與機電工程系教授

## 摘 要

本研究是一種選用 P 型與 K 型材質的碳化鎢刀片，磨成負稜主刃車刀後，針對碳纖維複合材料作切削研究。研究當中除了量測三軸切削力外，也做了刀片磨耗情形及工件表面光度等研究。而在研究開始之初，即先設計並製造出九種不同形狀的刀把，然後將刀片鎖在刀把上以磨成不同幾何形狀的刀片。此刀片包括負稜寬度，刀鼻半徑，切邊角，第一及第二側斜角...等，以作各種不同的切削實驗。結果顯示當側斜角一定，具有負稜的刀具切削力較低；且當側斜角為 20 度，第一及第二側斜角為負 10 度與正 10 度時，為一理想之刀具角度。另外 K 型負稜主刃車刀比 P 型車刀具有較佳的切削效果。

**關鍵詞：**車削，碳纖維複材，負稜主刃車刀

## I. Introduction

Composite materials are ideal for structural applications where high strength to weight and stiffness-to-weight ratios are required [1]. Carbon fiber reinforced plastics (CFRP) are also widely used in the structures of aircraft, robots and other machines because of their high strength to weight ratio, high stiffness-weight ratio, and high clamping capacity [2]. Although these materials have higher strength characteristics and lower density, relatively lower elastic stiffness is observed. For this reason, about 40 years ago experimental work was carried out on the thermal conversion of various organic precursor materials into carbon and graphite fibers and fabrics. The processing of the heavy-duty fibers set in different binders requires finishing by cutting for the production of finished components in virtually all processes [3]. König et al. [4] presented in spite of the near net shape production technology available for the processing, molding and curing of fiber reinforced plastics (FRP), these materials have to be machined. Sakuma et al. [5, 6] performed turning tests both on glass fiber-epoxy composite materials and carbon fiber-epoxy composite materials that contained unidirectional fibers. Several kinds of tool materials such as sintered carbides, ceramics, and cermets are used and the wear patterns and the wear land growth are analyzed. Ferreira et al. [7], showed that turning experiments were observed with the performance of different tool materials like ceramics, cemented carbide, cubic boron nitride (CBN), and diamond. During the tool wear tests, the machining forces and engine motor current were measured. Experimental results showed that only diamond tools are suitable for use in finishing turning. In rough turning, the carbide tools can be used in some retractions parameters. The wear of sintered-carbide tools and high-speed steel tools is very severe. Hence the cutting speed and feed rate of the machining operation should be selected carefully in the machining of carbon fiber-epoxy composite materials. Also, surface damage of the composite materials such as cracking and delimitation of the machined surface is severe and a low surface-roughness is not easily obtained [8, 9]. Machining characteristics of composites vary from metals due to the following reasons: (1) FRP is machinable in a limited range of temperature; (2) the low thermal conductivity causes

heat build up in the cutting zone during machining operation, since there is only little dissipation by the materials; (3) the difference in the coefficient of linear expansion between the matrix and the fiber gives rise to residual stresses and makes it difficult to attain high dimensional accuracy; (4) the change in physical properties by the absorption of fluids has to be considered while deciding to use a coolant [10].

Gallab [11] showed the cost of polycrystalline diamond tools (PCD) could be justified by using dry cutting; the relatively small built-up edge formed on the tool protects it from further wear by abrasion and micro cutting. Kim and Ehmann [12] demonstrated the knowledge of the cutting forces is one of the most fundamental requirements. This knowledge also gives very important information for cutter design, machine tool design and detection of tool wear and breakage. Hoshi and Hoshi [13] found that the apparent strength and the life of tool were increased if a small region of negative rake angle was ground on the main cutting edge and the contact length was controlled by a chip curler. A tool of this type was reported to decrease the energy by 15% and prolong tool life by roughly 20% compared with conventional tools [14]. Chang [15] illustrated that turning of medium carbon steel with chamfered main cutting edge tools could improve cutting efficiency. However, the effects of tool on turning of the CFRP were excluded from their discussion. The current paper presents a preliminary study on turning of on carbon fiber/epoxy laminates using chamfered main cutting edge carbide tools. The effects of tool geometry, cutting forces and chip formation have been studied.

## II. Theoretical Analysis

Composite materials are mainly molded parts, which require machining, especially face turning, to obtain the desired dimensional tolerances. For achieving the desired quality of the machined surface, it is necessary to understand the mechanism of material removal, the kinetics of machining, and the associated tribological processes affecting the performance of the cutting tools. Sreejith et al. [16] showed the wide difference in thermal properties of the fiber and matrix material and also the relatively poor thermal conductivity of composites makes it rather difficult to adopt any of the unconventional technique for machining of the polymeric composites.

Moreover, the unconventional processes cannot obtain shapes by traditional turning, drilling, and related processes, and therefore traditional material removing processes are most suited for machining polymeric composites. Since available data on the machining of such materials are relatively few and inconclusive, a detailed machining study was contemplated. Wang et al. [17] illustrated that chip formation, cutting forces, and the surface morphology in edge trimming of unidirectional graphite/epoxy was highly dependent on fiber orientation. Bhatnagar et al. [18] showed that in machining of fiber reinforced plastic (FRP) composite laminates; it can be assumed that the shear plane in the matrix depends only on the fiber orientation and not on the tool geometry.

Generally CFRP are heat insulating and abrasive in nature; hence the cutting tools have to encounter a relatively hazardous environment and undergo thermal associated wear processes. The available reports on cutting temperature and associated influences are mostly related to applications involving chamfered main cutting edge carbide tools. According to Chang [19], a basic force model of three dimensional turning glass fiber reinforced plastics (GFRP) process, which can predict the cutting forces for the case of turning with a chamfered main cutting edge, must consider nose radius  $R$ , cutting depth  $d$ , feed rate  $f$ , cutting speed  $V$ , the first side rake angle  $\alpha_{s1}$ , the second side rake angle  $\alpha_{s2}$ , and parallel back rake angle  $\alpha_b$  as shown in Table 1.

However, chamfered main cutting tools effects were not included in CFRP turning. The study was established in order to understand the behavior of CFRP during machining operations.

To obtain adequate strength of the cutting edge and to diminish the cutting forces, Hoshi & Hoshi [13] suggested that the value of the width  $W_e$  was constrained by the empirical equation (1)

$$W_e \cdot \cos C_s \leq f \quad (1)$$

where  $f$  is the federate,  $C_s$  is the side cutting edge angle.

According to Chang [15], the chamfered main cutting edge tool which can produce a secondary chip reduces the cutting force and aids the thermal dissipation. The results indicated that, for ease of chip flow, the side cutting edge angle  $C_s$  should fall in the range of  $20^\circ$  to  $40^\circ$ . The first side rake angle  $\alpha_{s1}$  and the second side rake angle  $\alpha_{s2}$  are fall into the range of  $-10^\circ$  to  $-30^\circ$  and  $10^\circ$  to  $30^\circ$ ,

respectively. Once  $C_s$ ,  $\alpha_{s1}$ , and  $\alpha_{s2}$  were determined, the feedrate was selected according to equation (1). The choice of the width of chamfer, the value of the negative side rake angle and the value of the nose radius greatly affect the ease of chip flow and the resultant surface roughness of the workpiece.

Based on the experimental results of Hoshi [13] and Chang [15], the turning tool geometries were selected then the tool holders were designed and manufactured. The basic model for a sharp corner tool with a chamfered main cutting edge tool ( $R=0$ ) is shown in Figs. 1 and 2.

### III. Experimental Method and Procedure

Experimental set up is shown in Figs. 3 and 4. Workpiece is observed in Fig 3b. to be held in the chuck of a lathe, and the cutters that were mounted with a dynamometer were employed for measuring the three axes compound of forces ( $F_H$ ,  $F_V$ , and  $F_T$ ). Dry cutting tests were carried out on a 7.5 HP PC-based CNC turning machine (SJ PC-3807, 20-4000rpm, brand name). In measuring the cutting forces, a Kistler 9257B three-component piezoelectric dynamometer was used with a data acquisition system that consisted of Kistler type 5807A charge amplifiers. An infrared detector was used to monitor the cutting tips, the temperature was recorded by the computer. All measured data were recorded by a data acquisition system (Keithley Metro byte-DAS1600) and analyzed by the control software (Easyest). The reliability of the measurement techniques was checked constantly by repeating the experiments. At the end of each cutting test, the tool flank wear ( $V_B$ ) was measured using a toolmaker's microscope.

#### 1. Workpiece

The work material used was  $0^\circ$ , unidirectional filament wound fiber of CFRP with Vinylester resin composite materials in the form of bars having a diameter of 40 mm and 500 mm length [20]. Some of the physical and mechanical properties of CFRP prior to carrying out the cutting experiments are as follows: nominal form is roving (continuous strand); density is  $1.7\sim 1.9 \text{ g/cm}^3$ ; thermal conductivity is  $0.21\sim 0.28 \text{ (k Cal/hr}^\circ\text{C)}$ ; fiber contain is 75 %; coefficient of thermal expansion is  $2\sim 9 \text{ (}10^{-6} \text{ }^\circ\text{C)}$ ; hardness is 55~60 Hs; tensile strength  $3.5\sim 4 \text{ (kg/cm}^2\text{)}$ ;

shear strength is 1.5~2 (kg/cm<sup>2</sup>); modulus tensile is 235~400 (kg/cm<sup>2</sup>).

## 2. Cutting Tools

For achieving cutting geometrical configurations, nine special cutting tool holders are machined so as to obtain the specified side cutting edge angle ( $C_s$ ), first and second side rake angle ( $\alpha_{s1}$  and  $\alpha_{s2}$ ) and also both K and P type carbide tip's which were grounded with a grinder. To have specified relief angle, negative rake angle and a certain chamfer width, the specifications are listed in Table 1. A total of 9 tool geometries could be made with various combinations of tool holders and tips. The dimensions of these tool holders and tool tips were inspected with a coordinate measuring machine so as to meet the specified requirements. Two kinds of tool materials [21] (Sandvik P10-S1P and K10-H1P) and various tool geometries were employed in the study. Tool composition, S1P (P type): WC 56%, TiC 19%, Ta(Nb)C 16%; H1P (K type) : WC 85.5%, TiC 7.5%, Ta(Nb)C 1%; and Co 1%. Oblique turning tests were carried out for each tool. However, for the purpose of comparing tool wear, all cutting test had a fixed time and the same cutting conditions.

## 3. Experimental Conditions

During the cutting test, the following conditions are assigned:

- A. dry cutting
- B. cutting velocity is 251 m/min (N=2000 rpm)
- C. cutting depth: d=1.5, 2.0 and 2.5mm
- D. feedrate: f=0.47mm/rev
- E. the tool holder was vertical to the feeding direction
- F. tool extension from the dynamometer:30mm

## IV. Results and Discussion

A series of preliminary tests were conducted to assess the effect of tool material on the tool wear, cutting forces, surface roughness and cutting temperature during the turning of CFRP.

### 1. The Cutting Forces

Chang [15], Fig. 5, showed in turning of plain carbon steels with chamfered main cutting edge tools resultant cutting force,  $F_r$ ; is about 15% less than that for unchamfered main cutting edge tool. The increase of the side rake angle  $\alpha_{s1}$  and  $\alpha_{s2}$ ,

decreases the total cutting force  $F_r$ ; in case of the constant of  $C_s$ . The increase of the side cutting edge angle,  $C_s$ , from 20° to 30°, decreases the cutting force. However, the cutting force would increase if the angle is increased from 30° to 40°, Figs. 5 to 11 are also to. Emphasize the different cutting situation between Carbon Steel and CFRP.

Figs. 6 (a, b, c) to 8 (a, b, c) indicate the experimental horizontal ( $F_H$ ), vertical ( $F_V$ ) and transversal ( $F_T$ ) cutting forces, respectively, which are obtained with the K type chamfered main cutting edge tools vs.  $\alpha_{s1}(\alpha_{s2})=10^\circ(-10^\circ)$ ,  $\alpha_{s1}(\alpha_{s2})=20^\circ(-20^\circ)$ , and  $\alpha_{s1}(\alpha_{s2})=30^\circ(-30^\circ)$  at  $C_s=20^\circ$  and  $R=0.1mm$  geometrical configurations.

Figs. 9 (a, b, c) to 11(a, b, c) indicate the experimental horizontal ( $F_H$ ), vertical ( $F_V$ ) and transversal ( $F_T$ ) cutting forces, respectively, which are obtained with the P type chamfered main cutting edge tools vs.  $\alpha_{s1}(\alpha_{s2})=10^\circ(-10^\circ)$ ,  $\alpha_{s1}(\alpha_{s2})=20^\circ(-20^\circ)$ , and  $\alpha_{s1}(\alpha_{s2})=30^\circ(-30^\circ)$  at  $C_s=20^\circ$  and  $R=0.1 mm$  geometrical configurations.

The observed results shown in the Figures imply that:

### A. Comparing turning of carbon steel and CFRP workpiece:

A turning of CFRP materials with chamfered main cutting edge tools decreases the cutting forces  $F_H$ ,  $F_V$  and  $F_T$ . In Figs. 6 to 11, the results show good agreement with Chang and Fuh in turning medium carbon steel [15].

The cutting force values are observed in Figs. 6 to 11, to be the smallest in the case of  $C_s=20^\circ$ ,  $\alpha_{s1}(\alpha_{s2})=10^\circ(-10^\circ)$ ,  $R=0.1mm$ . The reason is due to decrease of the fiber chip, and more obvious and smoother formation and flow of the powder chip. Especially, decreasing the  $C_s$ , means shorter contact length between the chip and tool, which caused the cutting CFRP efficiency to increase and the difficulty of chip formation to decrease, as shown in Section IV(2), Figs. 13 (a, b and c)-14 (a, b and c).

### B. Comparing different P and K type of chamfered main cutting edge carbide tools:

Due to severe edge chipping, the cutting forces for the chamfered main cutting edge of P type carbide tools were much higher than using chamfered main cutting edge of K type carbide tools.

## 2. The Shape of Chips

Chang and Fuh [15] showed, when turning of medium carbon steel with chamfered main cutting edge tools, the secondary chip is formed more obviously and has flowed more easily under the situation of  $C_S=30^\circ$ ,  $\alpha_{S1}=-30^\circ$  and  $\alpha_{S2}=30^\circ$ . Producing a secondary chip in the case of  $C_S=20^\circ$ ,  $\alpha_{S1}=-10^\circ$  and  $\alpha_{S2}=10^\circ$  is rather difficult, as shown in Figs. 12 (a, b, c).

Knowing the relation between the main chips and secondary chips, the different tool geometrical configurations on various side rake angles and cutting edge angles are first attempted to be understood. Nine kinds of tools were used in turning the CFRP workpiece in the same cutting condition. The different chip shapes with K type tool and P type tool are provided in Figs. 13 (a, b, c) and Figs. 14 (a, b, c) respectively.

**A.** producing a secondary chip in these nine kinds of chamfered main cutting edge tools is rather difficult and it is formed unobviously.

**B.** In Fig. 13a, the powder chip is formed more obviously and has flowed more easily under the situation of  $C_S=20^\circ$ ,  $\alpha_{S1}=-10^\circ$  and  $\alpha_{S2}=10^\circ$ .

**C.** For producing the fiber chips, in Figs. 13 to 14, the fiber chip more formed obviously when we used the chamfered main cutting edge of P type tool, and the  $C_S$  from  $20^\circ$  to  $40^\circ$ ,  $\alpha_{S1}=-30^\circ$  and  $\alpha_{S2}=30^\circ$ .

**D.** In turning of CFRP with chamfered main cutting edge tools, no secondary chips are observed for all kinds of the tool, in Figs. 13 to 14. In the turning of CFRP, the chips are both powder and fiber, it is difficult to observe the shear zone, and the secondary flows were not observed.

## 3. The Temperature of Tip's Surface

Cutting tools usually have higher temperature over the three distinct zones. Namely these are the cutting nose, the secondary grooving zone, and the depth of cut region or primary cutting edge.

Knowing the temperature of cutting tools and how these chamfered main cutting edge tools decrease the temperature of the tool tip surface, Chang [15] demonstrated that in turning medium carbon steel, the temperature of the main chip rises to nearly  $300^\circ\text{C}$ , but the tip's surface temperature is not over  $200^\circ\text{C}$ .

**A.** Fig. 15 showed the tip's surface temperature as a function of various side cutting edge angle  $C_S$  for different  $\alpha_{S1}$  ( $\alpha_{S2}$ ), and P or K type of chamfered

main cutting edge carbide tools respectively. In Figs. 15, it can be seen that using the chamfered main cutting tools in turning CFRP materials, the tip's surface temperature is not over  $190^\circ\text{C}$ , and at nose radius  $R=0.1\text{mm}$ , the tip's surface temperature is the lowest, and the cutting forces are also the smallest.

**B.** Fig. 15, indicates the tip's surface temperature increase according to  $C_S$  from  $20^\circ$  to  $40^\circ$ . For the  $C_S$  of nearly  $40^\circ$ , the effect of larger contact area on the tool-tip edge, the majority of chip being fiber and the larger normal stress on the cutting edge, is the cutting forces increase significantly.

## 4. The Wear of Tips

**A.** The chamfered main cutting edge P and K type of turning tool have been ground according to various designed specifications, but the unchamfered main cutting edge with sharpness turning tool ( $R=0$ ) has more crater and flank wear than the above tool after face turning time of about 10 min, as shown in Figs. 16 to 18. The chamfered main cutting edge tools are better and more resistant than those of the unchamfered main cutting edge tools.

**B.** The chamfered main cutting edge tool with the nose radius ( $R=0.1\text{mm}$ ) has the least wear among various tools as observed in Figs. 17 (a,b,c) and 18(a,b,c) by comparing the wear of the tips. Additionally, the chamfered main cutting edge with sharp tool ( $R=0$ ) has a medium level of wear, and unchamfered tool ( $R=0$ ) has the largest. The reasons are that the formal tools possess a lower oxidation wear associated with low temperature at chamfered main cutting edge and the chip is produced more easily and these tools have the smaller cutting forces among the other tools.

**C.** K type of chamfered main cutting edge carbide tools sustained tool wear less than the P type chamfered main cutting edge carbide tools. This is undoubtedly due to K type of tools superior hardness and wear resistance, as well as low coefficient of friction together with high thermal conductivity. On the other hand the P type of tools suffered from excessive crater wear and chipping.

## 5. The Surface Roughness of the Workpiece

To measure the surface roughness of workpiece, a measuring machine Tokyo Seimitisu surfcom (Brand name) was used as Fig. 4a. In the measure of each workpiece was 2.5mm in the linear direction, while the data were recorded three times at different sections.

The results were then averaged.

The surface roughness of workpiece Ra ( $\mu\text{m}$ ) vs  $C_s$ , is shown in Fig. 19 for various  $\alpha_{s1}$  and  $\alpha_{s2}$  at  $R=0.1\text{mm}$ , chamfered main cutting P and K tool.

**A.** For constant  $C_s$ , in Fig. 19, decreasing the side rake angle  $\alpha_{s1}$  and  $\alpha_{s2}$ , decreases the surface roughness Ra.

**B.** In Fig. 19, in the case of  $C_s=20^\circ$ ,  $\alpha_{s1}(\alpha_{s2})=-10^\circ$  ( $10^\circ$ ) at  $R=0.1\text{mm}$ , the values of surface roughness Ra is the smallest.

## V. Conclusions

A series of preliminary tests were conducted to assess the effect of tool geometries of P and K type of chamfered main cutting edge carbide tool on the tool wear, cutting forces, workpiece surface roughness, and cutting temperature during the turning of CFRP. Due to the K type tool's with superior hardness and wear resistance, as well as low coefficient of friction together with high thermal conductivity, it was shown that chamfered main cutting edge K type carbide tools sustained the least tool wear, compared to unchamfered K and P type of tool. The cutting forces, cutting temperature and workpiece surface roughness for the chamfered main cutting edge of P type carbide tools in turning were much higher than using chamfered main cutting of K type carbide tools. On the other hand, the K type of chamfered main cutting carbide tools achieved from lower crater wear and chipping K type of chamfered main cutting edge tools with  $C_s$  equals  $20^\circ$ , the conditions  $f=.45\text{mm/rev}$ ,  $\alpha_{s1} = -10^\circ$ ,  $\alpha_{s2} = 10^\circ$  and nose radius  $R=0.1\text{mm}$ , produced the lower cutting forces, lower cutting temperature and lower tip wear.

Chamfered main cutting edge tools have the advantage of a limited chip contact length within the tool face. If the chamfer width is suitable, the effect not only diminishes the cutting forces, cutting temperature, and tool wear but also improves the surface roughness of the workpiece. Another important factor in CFRP machining is workshop environment; the powder and fiber chip generated irritates the skin and is dangerous for the health. The use of a vacuum cleaner, and safety protections for the operators is highly recommended.

## Nomenclature

$A$	shear area ( $\text{mm}^2$ )
$d$	depth of cut ( $\text{mm}$ )
$f$	feedrate ( $\text{mm/rev}$ )
$F_H$	horizontal cutting force ( $N$ )
$F_T$	transverse cutting force ( $N$ )
$F_V$	vertical cutting force ( $N$ )
$R$	nose radius ( $\text{mm}$ )
$r$	main cutting edge radius ( $\text{mm}$ )
$R_a$	arithmetic average roughness ( $\mu\text{m}$ )
$T$	cutting time ( $\text{min}$ )
$T_e$	temperature ( $^\circ\text{C}$ )
$t_w$	depth of tool wear ( $\text{mm}$ )
$V$	cutting velocity ( $\text{m/min}$ )
$V_f$	feed rate
$W_e$	chamfering width ( $\text{mm}$ )
$C_s$	side cutting edge angle ( $\text{rad}$ )
$\alpha_e$	effective rake angle ( $\text{rad}$ )
$\alpha_{s1}$	first side rake angle ( $\text{rad}$ )
$\alpha_{s2}$	second side rake angle ( $\text{rad}$ )
$\phi_e$	effective shear angle ( $\text{rad}$ )
$\sigma_y$	yield normal stress ( $\text{MN/mm}^2$ )
$\tau_y$	yield shear stress ( $\text{MN/mm}^2$ )
$\tau_s$	shear stress ( $\text{MN/mm}^2$ )

## References

- [1] H. Hocheng, H.Y. Tsai, J. J. Shiue, and B. Wang, "Feasibility study of Abrasive Waterjet Milling of Fiber-reinforced plastics", J. of Manufacturing Science and Engineering, ASME, vol. 119, 1997, pp.133-142
- [2] K. S. Kim, D.G. Lee, Y. K. Kwak and S. Namgung, "Machinability carbon-fiber-epoxy composite materials in turning", J. of Materials Processing Technology, vol. 32,1992, pp.553-570
- [3] P. Dennis, "Machining fiber-reinforced plastics", Industrial diamond review, vol.547 (51), pp. 288-291, 1991
- [4] W. Konig, C.H. Wulf, P. Grass, H. Willerscheid, "Machining of fiber reinforced plastics", Ann CIRP, vol. 34(2), 1985, pp. 537-548
- [5] K. Sakuma and M. Seto, "Tool wear in cutting glass-fiber-reinforced plastics", Bulletin of the JSME, vol. 26(218), 1983, pp. 1420-1427

- [6] K. Sakuma, M. Seto and M. Taniguchi, "Tool wear in cutting carbon-fiber-reinforced plastics", Bulletin of the JSME, vol. 28(245), 1985, pp. 2781-2788
- [7] J.R. Ferreira, N.L. Coppini and F. L. Neto, "Characteristics of carbon-carbon composite turning", J. of Materials Processing Technology, vol. 109, 2001, pp. 65-71
- [8] K.S. Kim, D.G. Lee and Y.K. Kwak, "Cutting (milling) characteristic's of carbon fiber/epoxy composites", Trans. of Korean Soc. Mechanical Engineering, vol. 14(1), 1990, pp. 237-240
- [9] G. Linbin, "Handbook of composites", Van Nostrand Reinhold, New York, pp. 625-629, 1982
- [10] S.K. Malhotra, "Some studies on drilling of fibrous composite", J. of Materials processing Technology, 24, 1990, pp. 292-300
- [11] M. EL-Gallab, and M. Sklad, "Machining of Al/SiC particulate metal-matrix composites, part I: Tool performance", J. of Materials Processing Technology, vol. 83, 1998, pp.151-158
- [12] H. S. Kim and K. F. Ehmann, "A cutting force model for face milling operations", Int. J. Mach. Tool Des., Res., vol. 33, 1993, pp. 651-673
- [13] K. Hoshi and T. Hoshi, "Silver-white chip (SWC) cutting tools", in:metal cutting technology, Kogyo Chosakai Publishing, Japan, 1969, pp. 87-104
- [14] M. C. Shaw, "Tool materials, in metal cutting principles", Oxford University Press, USA, 1984, pp. 335-367
- [15] C.S. Chang and K. H. Fuh, "Prediction of the cutting forces for chamfered main cutting edge tools", In., J. of Mach. Tools & Manu., De., Res. and Appl., vol. 35(1),1995, pp. 1559-1586
- [16]P.S. Sreejith, R. Krishnamurthy, S.K. Malhotra and K. Narayanasamy, "Evaluation of PCD tool performance during machining of carbon /phenolic ablative composites", J. of Materials processing Technology, vol. 104, 2000, pp. 53-58
- [17]D.H. Wang, M. Ramulu and D. Arola, " Orthogonal cutting mechanisms of Graphite /Epoxy composite. Part1: unidirectional laminate", In., J. of Mach. Tools & Manu., De., Res. and Appl., vol. 35(12),1995, pp. 1623-1638
- [18] N. Bhatnagar, N. Ramakrishnan, N.K. Naik and R. Komanduri,"On the machining of fiber reinforced plastic(FRP) composite laminates", In., J. of Mach. Tools & Manu., De., Res. and Appl., vol. 35(5), 1995, pp. 701-716
- [19] C.S. Chang, "Turning of glass fiber reinforced plastics (GFRP) composite materials with chamfered main cutting edge carbide tools", 8<sup>th</sup> International Conf. on Manufacturing & Management, Australia, 2004, pp. 964-983
- [20] C.C. Liu,"FRP and GTI composites", Golden Talent Industries Co. Ltd., Hsin-Chu, Taiwan, R.O.C., 2002
- [21] K. J. A. Brookes, "World directory and handbook of hard metals, 5th edition, published by International carbide data hand book", United Kingdom, pp. D172-1752, 1992

## Acknowledgement

This work was supported by National Science Council , Taiwan, under grant number NSC 92-2622-E-197-002-CC3.

## Appendix

Coefficients of the tool having a sharp corner

(R=0) without tool wear

$$t_1 = f \cos C_S \quad (A1)$$

$$t_2 = W_e \cos \alpha_{S1} \quad (A2)$$

$$t_3 = t_1 - t_2 \quad (A3)$$

$$f_1 = f - W_e \cos \alpha_{S1} \quad (A4)$$

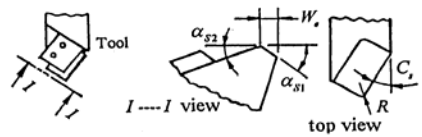
$$b = d / \cos C_S \quad (A5)$$

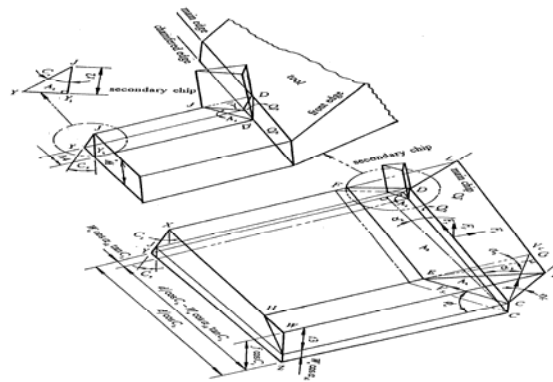
$$b_4 = t_2 \tan C_S \quad (A6)$$

$$b_2 = b - b_4 \quad (A7)$$

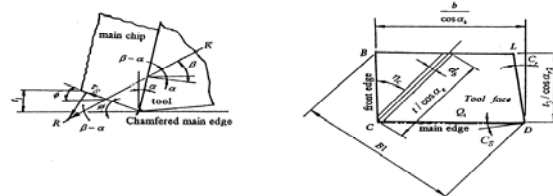


Table 1 Tool geometrical specifications

Side cutting edge angle, $C_S$	Tool No.	Side rake angle $(\alpha_{s1}, \alpha_{s2})$	Nose radius ( R ), unit : mm 	Carbide tool
20°	1	-10° , 10°	Sharp (R=0), chamfered (R=0, R=0.1)	P10, K10
20°	2	-20° , 20°	Sharp (R=0), chamfered (R=0, R=0.1)	P10, K10
20°	3	-30° , 30°	Sharp (R=0), chamfered (R=0, R=0.1)	P10, K10
30°	4	-10° , 10°	Sharp (R=0), chamfered (R=0, R=0.1)	P10, K10
30°	5	-20° , 20°	Sharp (R=0), chamfered (R=0, R=0.1)	P10, K10
30°	6	-30° , 30°	Sharp (R=0), chamfered (R=0, R=0.1)	P10, K10
40°	7	-10° , 10°	Sharp (R=0), chamfered (R=0, R=0.1)	P10, K10
40°	8	-20° , 20°	Sharp (R=0), chamfered (R=0, R=0.1)	P10, K10
40°	9	-30° , 30°	Sharp (R=0), chamfered (R=0, R=0.1)	P10, K10



(a)



(b)

Fig.1 (a) (b) basic model of the chamfered main cutting edge tool,  $f > R$ ,  $R = 0$

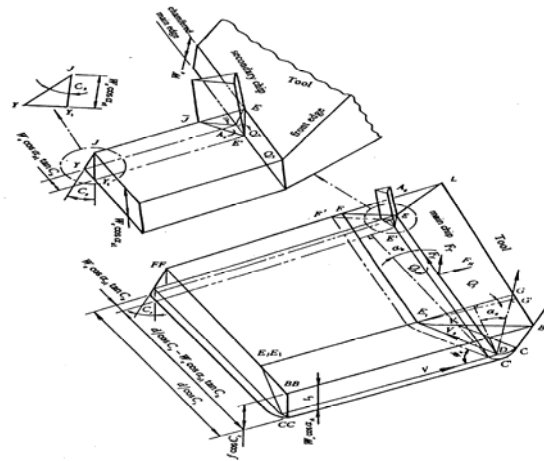
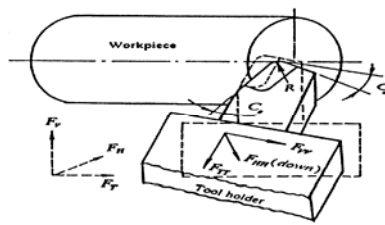
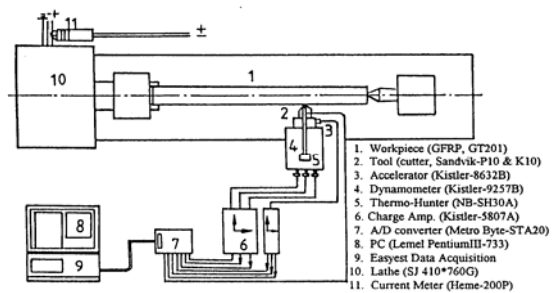


Fig. 2 Basic model of the chamfered main cutting edge,  $R \neq 0$ ,  $R < r$



(a)



(b)

Fig.3 Experimental set-up



Fig.4 The experimental set-up (a) surface roughness measuring, (b) dynamometer, tool and GFRP workpiece.

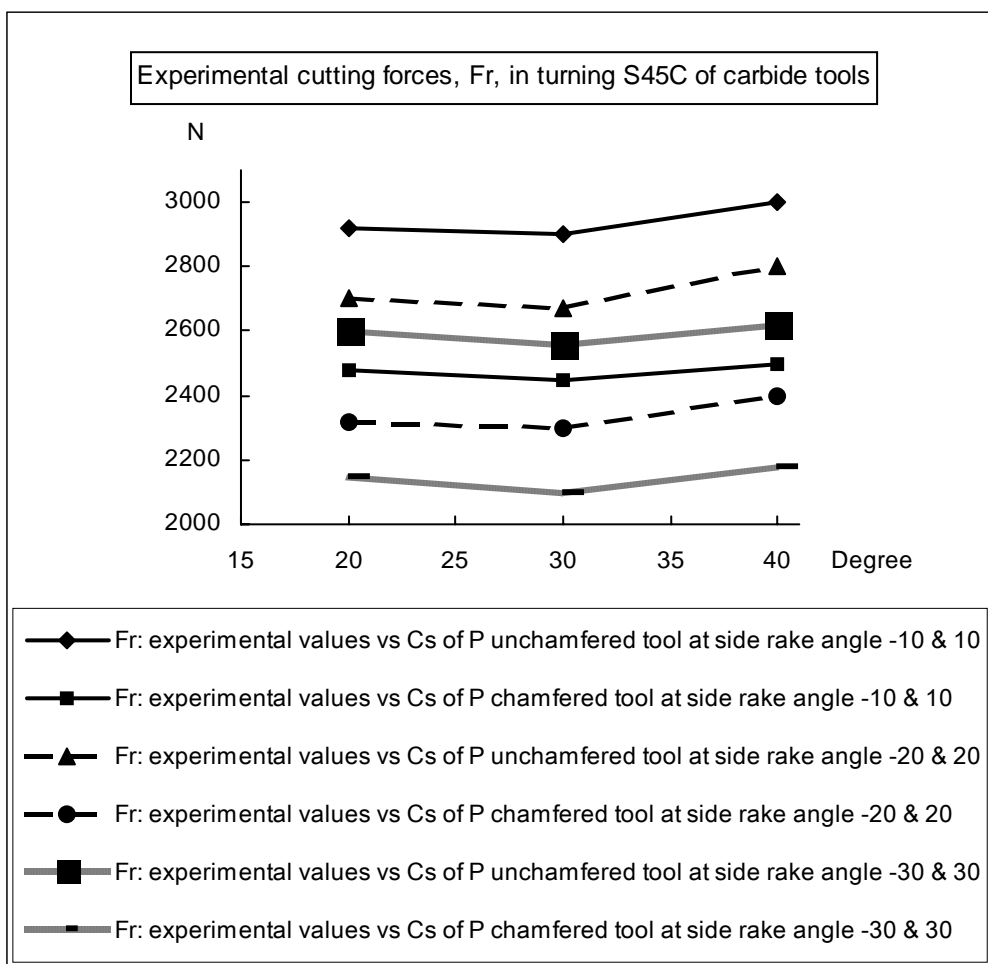
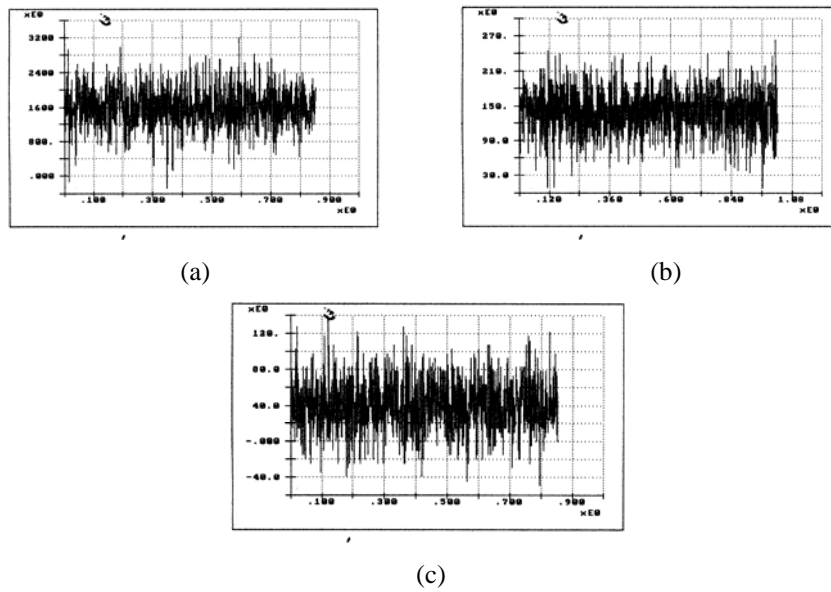
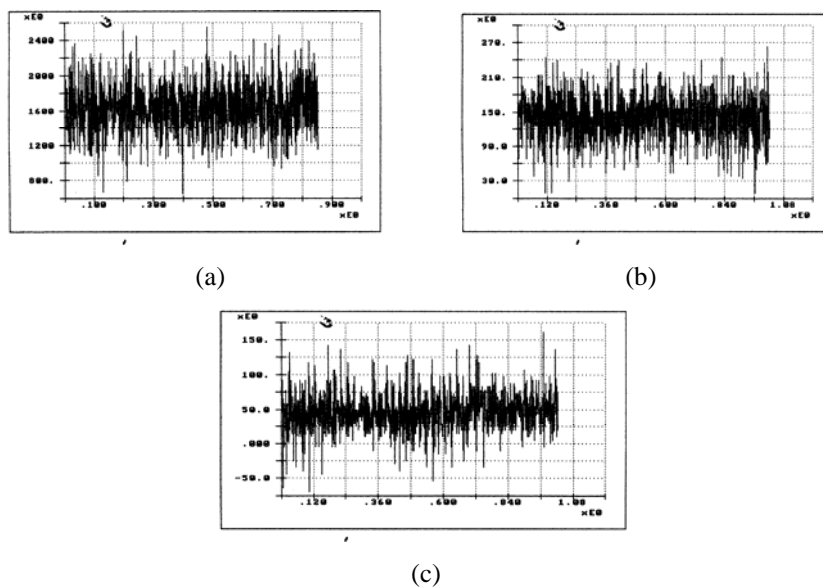


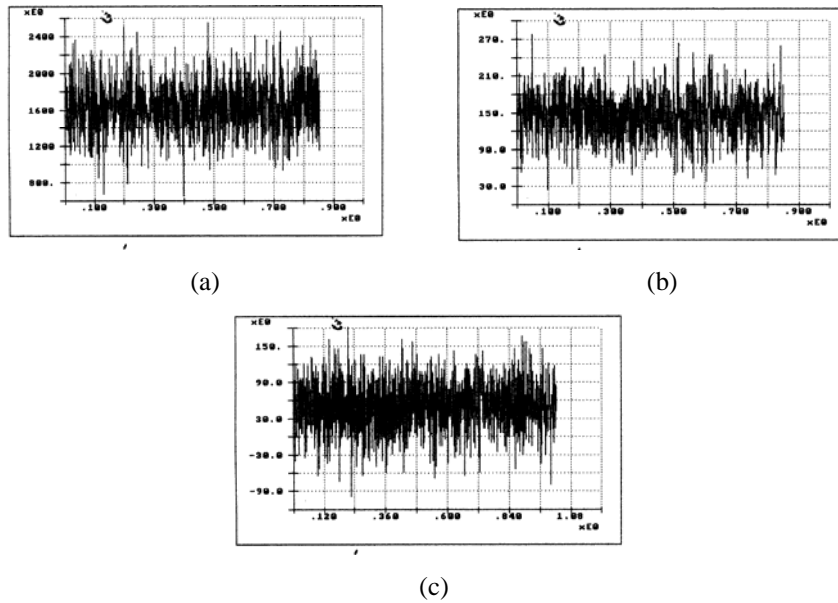
Fig. 5 The resultant cutting forces  $F_r$  (N), vs.  $C_s$  ( $^\circ$ ) for different values of  $\alpha_{s1}$  and  $\alpha_{s2}$  at  $d=2.5$ mm,  $f=.33$ mm/rev,  $R=0$ , and  $V=145$ m/min (medium carbon steel)



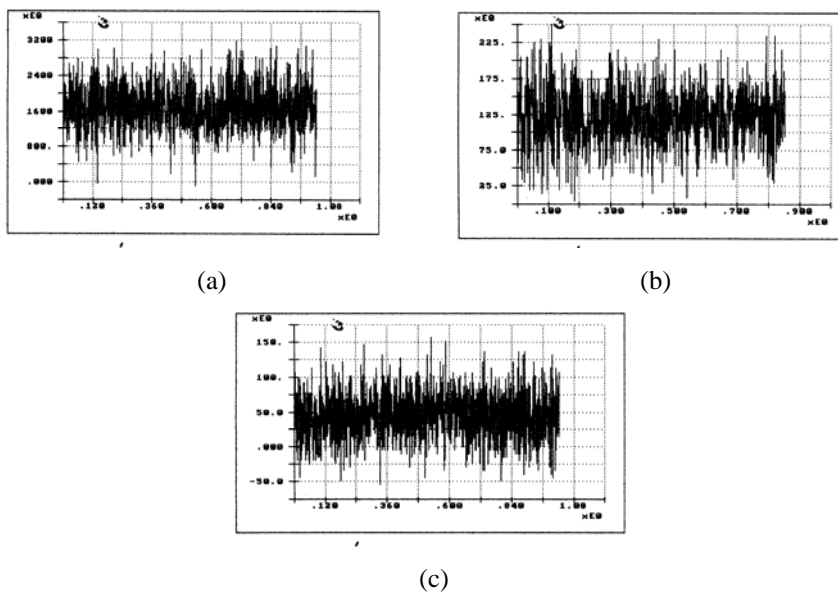
Figs. 6 The experimental cutting forces (a) horizontal ( $F_H$ ), (b) vertical ( $F_V$ ), and (c) transversal ( $F_T$ ) with K type chamfered edge tools at  $C_S = 20^\circ$ ,  $\alpha_{S1}(\alpha_{S2}) = -10^\circ$  ( $10^\circ$ ),  $R=0.1\text{mm}$ ,  $d=2.5\text{mm}$ ,  $f=.457$  mm/rev and  $V=252\text{m/min}$  (CFRP)



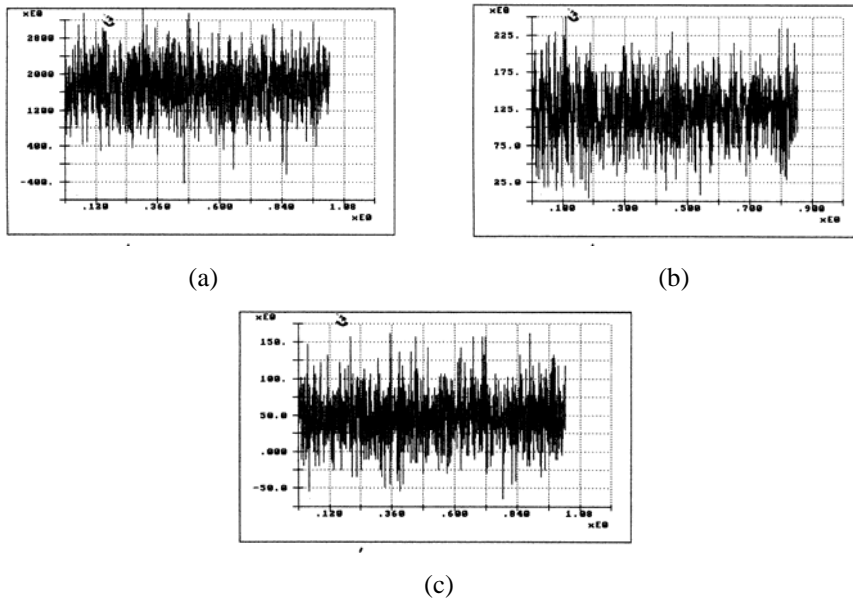
Figs. 7 The experimental cutting forces (a) horizontal ( $F_H$ ), (b) vertical ( $F_V$ ) and (c) transversal ( $F_T$ ) with K type chamfered edge tools at  $C_S = 20^\circ$ ,  $\alpha_{S1}(\alpha_{S2}) = -20^\circ$  ( $20^\circ$ ),  $R=0.1\text{mm}$ ,  $d=2.5\text{mm}$ ,  $f=.457$  mm/rev and  $V=252\text{m/min}$  (CFRP)



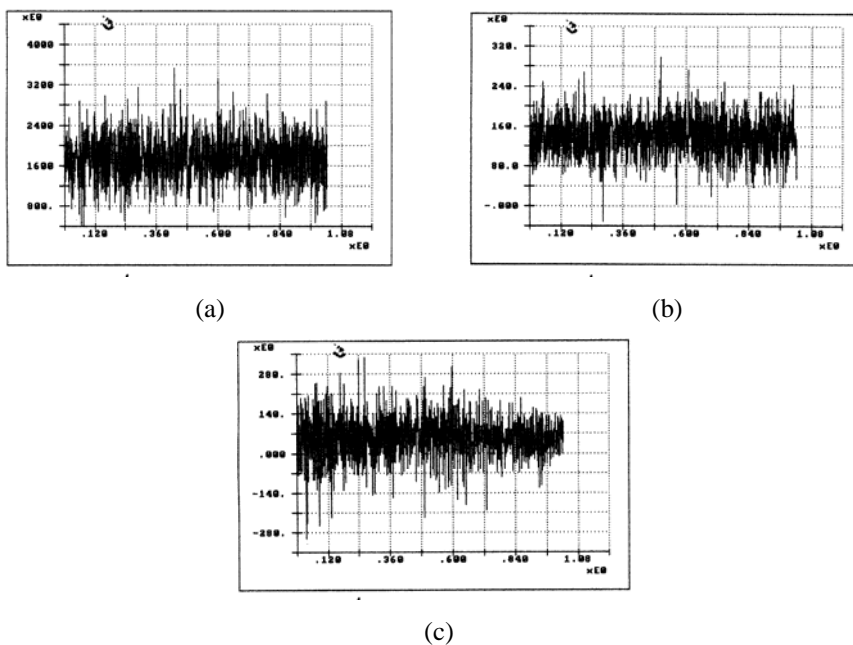
Figs. 8 The experimental cutting forces (a) horizontal ( $F_H$ ), (b) vertical ( $F_V$ ) and (c) transversal ( $F_T$ ) with K type chamfered edge tools at  $C_S=20^\circ$ ,  $\alpha_{S1}(\alpha_{S2})=-30^\circ(30^\circ)$ ,  $R=0.1\text{mm}$ ,  $d=2.5\text{mm}$ ,  $f=.457\text{ mm/rev}$  and  $V=252\text{m/min}$  (CFRP)



Figs. 9 The experimental cutting forces (a) horizontal ( $F_H$ ), (b) vertical ( $F_V$ ) and (c) transversal ( $F_T$ ) with P type chamfered edge tools at  $C_S=20^\circ$ ,  $\alpha_{S1}(\alpha_{S2})=-10^\circ(10^\circ)$ ,  $R=0.1\text{mm}$ ,  $d=2.5\text{mm}$ ,  $f=.457\text{ mm/rev}$  and  $V=252\text{m/min}$  (CFRP)



Figs. 10 The experimental (a) horizontal ( $F_H$ ), (b) vertical ( $F_V$ ) and (c) transversal ( $F_T$ ) cutting forces with P type chamfered edge tools at  $C_S=20^\circ$ ,  $\alpha_{S1}(\alpha_{S2})=-20^\circ(20^\circ)$ ,  $R=0.1\text{mm}$ ,  $d=2.5\text{mm}$ ,  $f=.457\text{ mm/rev}$  and  $V=252\text{m/min}$  (CFRP)



Figs. 11 The experimental cutting forces (a) horizontal ( $F_H$ ), (b) vertical ( $F_V$ ) and (c) transversal ( $F_T$ ) with P type chamfered edge tools at  $C_S=20^\circ$ ,  $\alpha_{S1}(\alpha_{S2})=-30^\circ(30^\circ)$ ,  $R=0.1$ ,  $d=2.5\text{mm}$ ,  $f=.457\text{ mm/rev}$  and  $V=252\text{m/min}$  (CFRP)

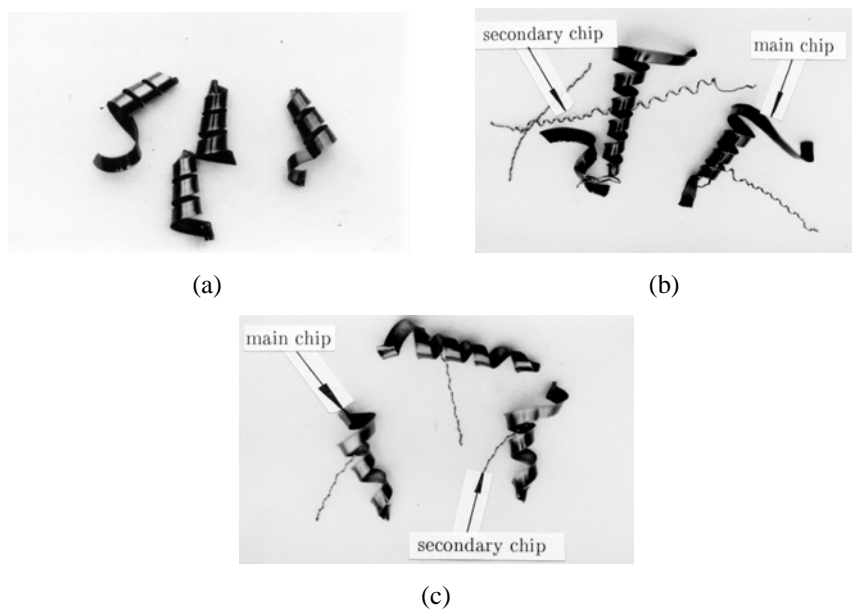


Fig 12 Shape of chips (a)  $\alpha_{s1}(\alpha_{s2}) = -10^\circ(10^\circ)$ , (b)  $\alpha_{s1}(\alpha_{s2}) = -20^\circ(20^\circ)$ , and (c)  $\alpha_{s1}(\alpha_{s2}) = -30^\circ(30^\circ)$  at  $C_s=30^\circ$ ,  $d=2.5$  mm,  $R=0.1$ mm, and  $V=140-148$  m/min (carbon steel), 50X

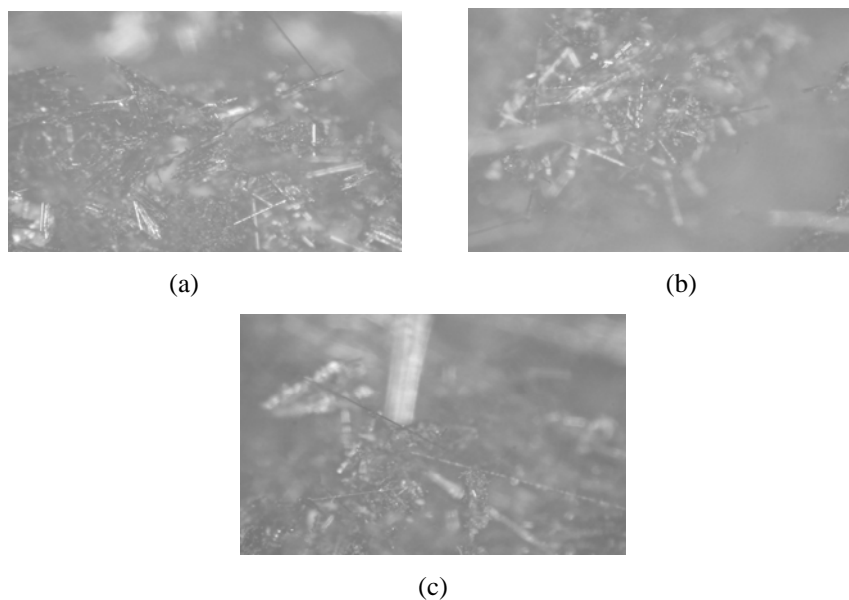


Fig. 13 Shape of chips with K type tool, (a)  $\alpha_{s1}(\alpha_{s2}) = -10^\circ(10^\circ)$ , (b)  $\alpha_{s1}(\alpha_{s2}) = -20^\circ(20^\circ)$ , and (c)  $\alpha_{s1}(\alpha_{s2}) = -30^\circ(30^\circ)$  at  $C_s=20^\circ$ ,  $d=2.5$  mm,  $R=0.1$ mm, and  $V=252$  m/min (CFRP), 50X

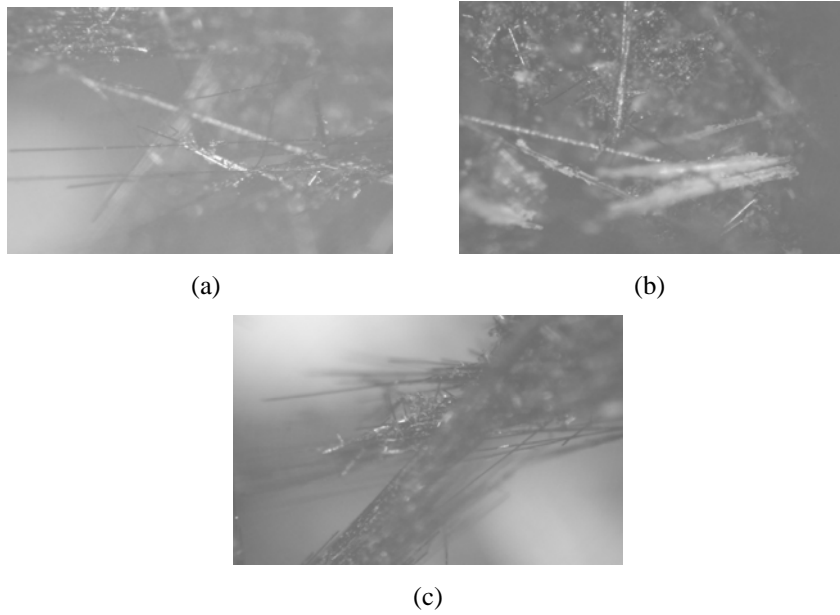


Fig. 14 Shape of chips with P type tool, (a)  $\alpha_{s1}(\alpha_{s2}) = -10^\circ(10^\circ)$ , (b)  $\alpha_{s1}(\alpha_{s2}) = -20^\circ(20^\circ)$ , and (c)  $\alpha_{s1}(\alpha_{s2}) = -30^\circ(30^\circ)$  at  $C_s=20^\circ$ ,  $d=2.5$  mm,  $R=0.1$ mm, and  $V=252$  m/min (GFRP), 50X



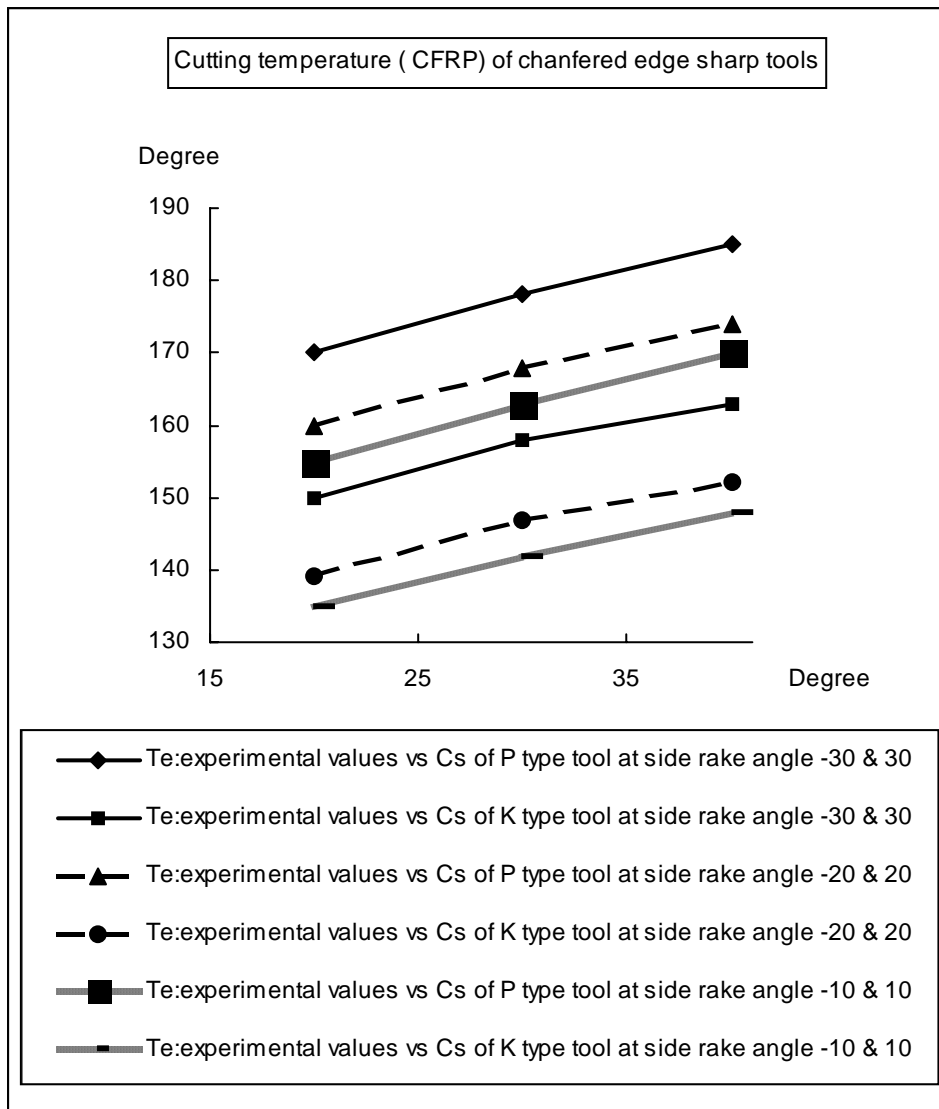
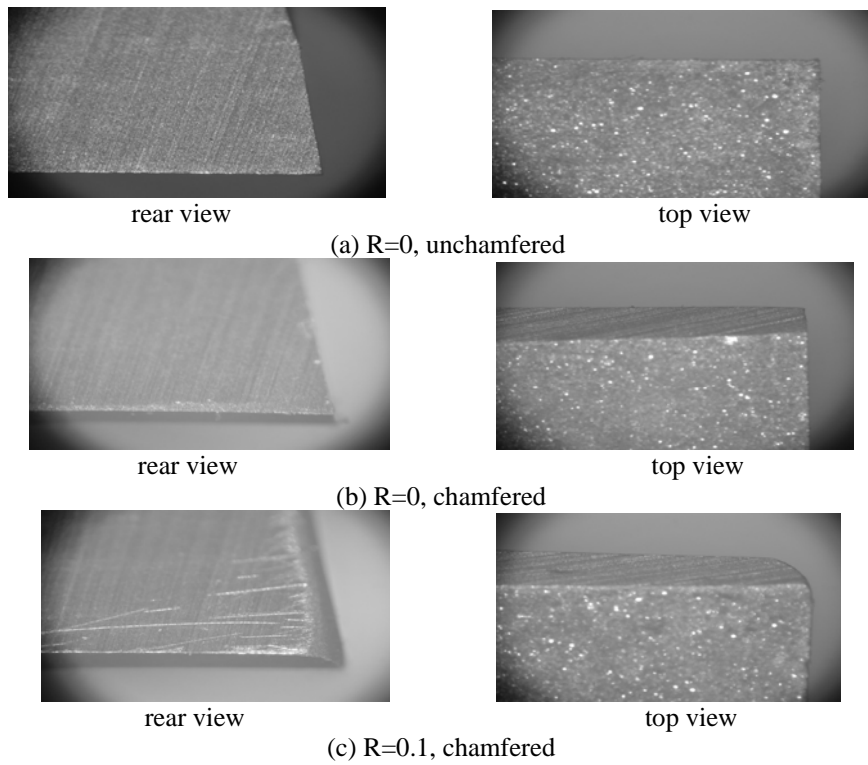
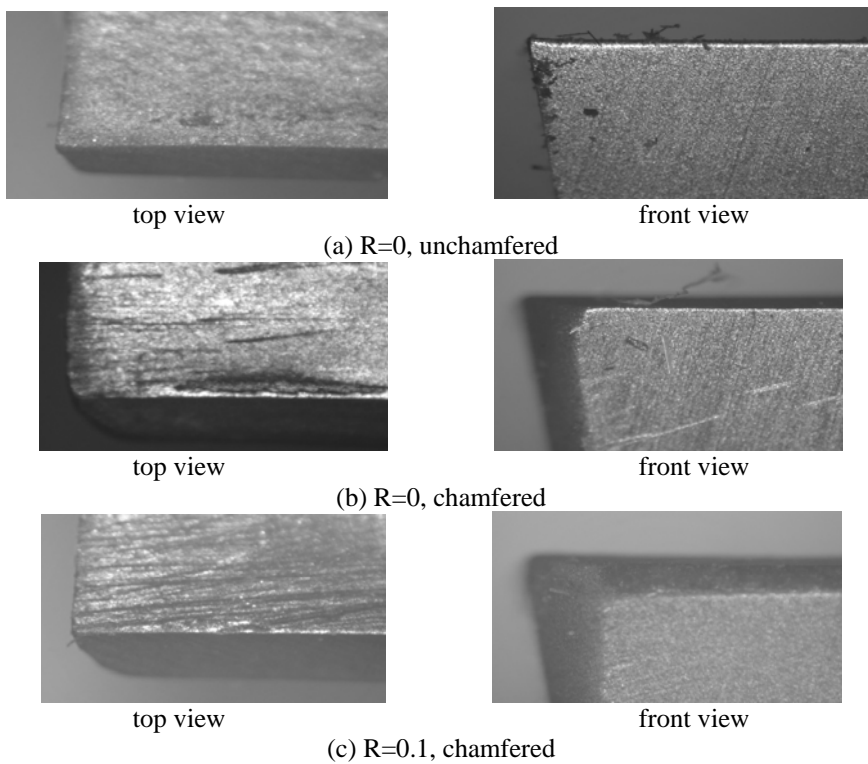


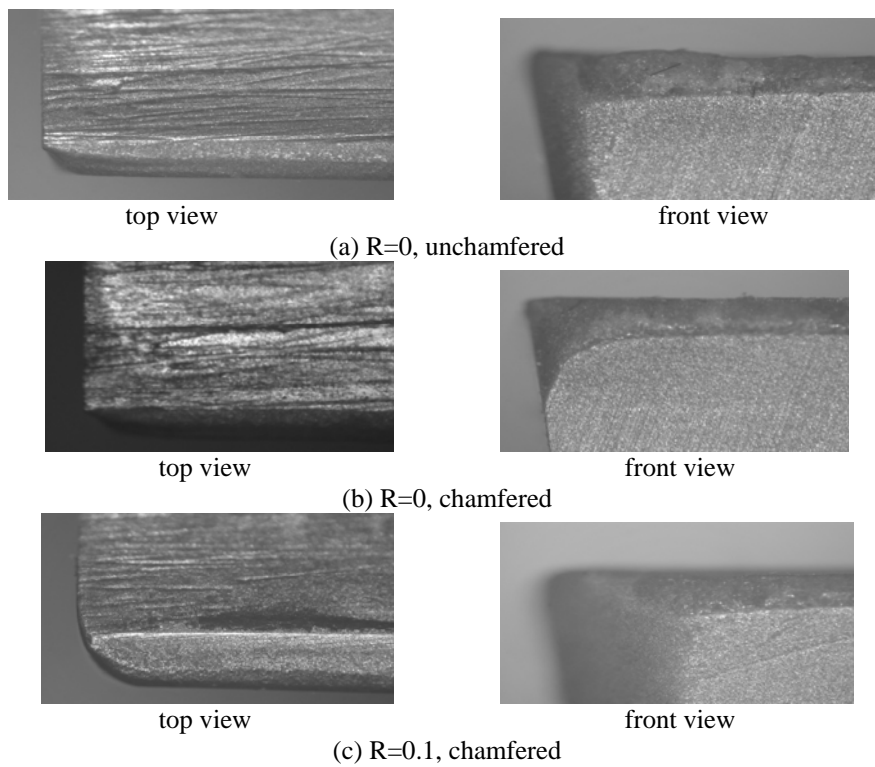
Fig. 15 The cutting temperature  $T_e$  (°C) versus side cutting angle  $C_s$ ,  $\alpha_{s1}$  and  $\alpha_{s2}$  of chamfered cutting edge P and K type tools at  $R=0.1$  mm,  $d=2.5$  mm,  $f=0.25$  mm/rev and  $V=252$  m/min



Figs. 16 The new K type tool view of (a), (b) and (c) with  $C_S=20^\circ$ , and  $\alpha_{S1}(\alpha_{S2}) = -20^\circ$  ( $20^\circ$ ) respectively (80X)



Figs. 17 The worn K type tool view of (a), (b) and (c) with  $C_S=20^\circ$ , and  $\alpha_{S1}(\alpha_{S2}) = -20^\circ$  ( $20^\circ$ ), at cutting time 10 min,  $d=2$  mm,  $f=0.24$  mm/rev and  $V=252$  m/min respectively (80X)



Figs. 18 The worn P type tool view of (a), (b) and (c) with  $C_S=20^\circ$ , and  $\alpha_{S1}(\alpha_{S2})=-20^\circ$  ( $20^\circ$ ), at cutting time 10 min,  $d=2$  mm,  $f=0.24$  mm/rev and  $V=252$ m/min respectively

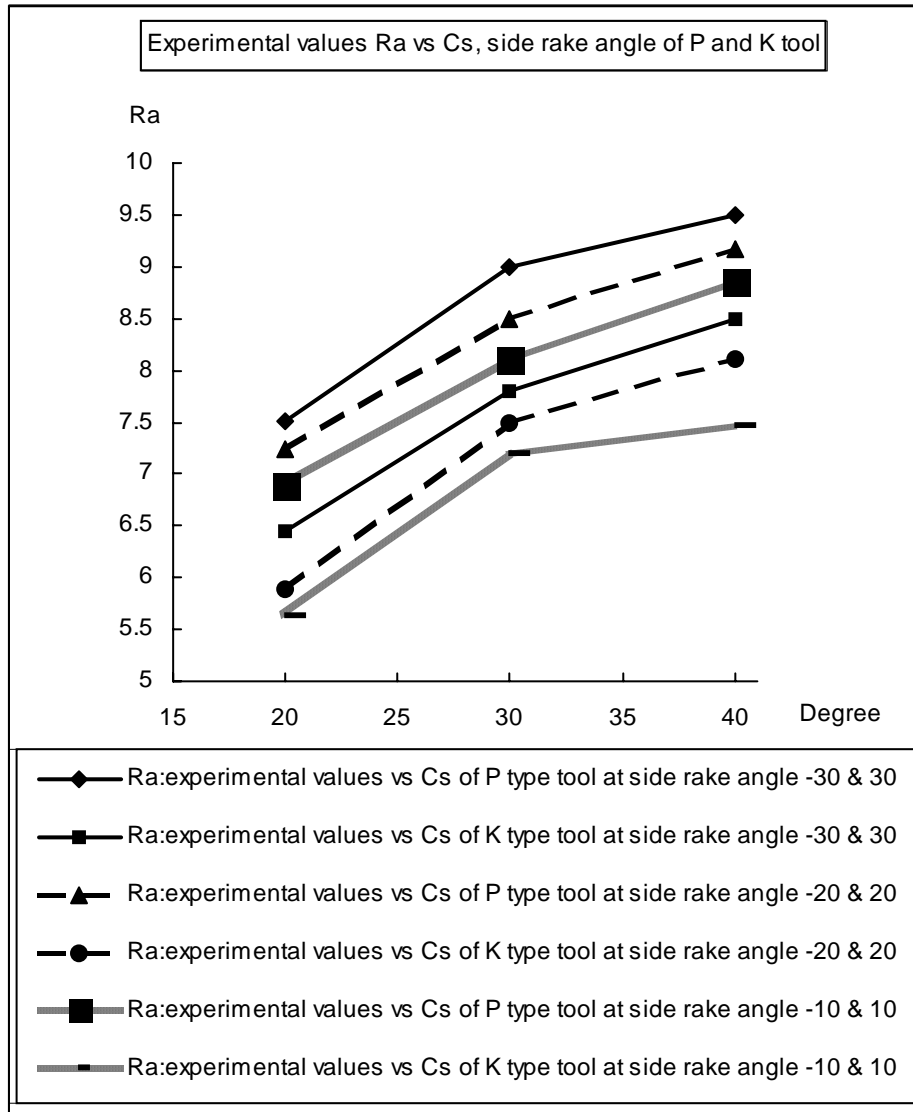


Fig. 19 The surface roughness Ra vs side cutting angle  $C_s$ ,  $\alpha_{s1}$  and  $\alpha_{s2}$  (°) of P and K type chamfered cutting edge tools at  $d=2.5$  mm,  $f=0.25$  mm/rev and  $V=252$  m/min